

Atomic-Structure-Dependent Schottky Barrier at Epitaxial Pb/Si(111) Interfaces

D. R. Heslinga,⁽¹⁾ H. H. Weitering,⁽²⁾ D. P. van der Werf,^{(1),(a)} T. M. Klapwijk,⁽¹⁾ and T. Hibma⁽²⁾

⁽¹⁾Department of Applied Physics, University of Groningen, Nijenborgh 18, 9747 AG Groningen, The Netherlands

⁽²⁾Department of Inorganic Chemistry, University of Groningen, Nijenborgh 16, 9747 AG Groningen, The Netherlands

(Received 27 December 1989)

The Schottky barrier of Pb grown epitaxially on *n*-type Si(111) has been studied. Two structures can be formed, which differ only in the arrangement of the first layer of Pb and Si atoms at the interface. One, a Si(111)(7×7)-Pb structure, has a Schottky-barrier height of 0.70 eV. The other a Si(111)(√3×√3)R30°-Pb structure, has a barrier height of 0.93 eV. These results emphasize the importance of the local electronic structure for Schottky-barrier formation at ordered interfaces.

PACS numbers: 73.30.+y, 73.40.-c

The search for the fundamental mechanisms determining Schottky-barrier formation at metal-semiconductor interfaces has been strongly influenced by Tung's discovery of the relation between atomic structure and Schottky-barrier height at epitaxial NiSi₂/Si(111) contacts.¹ A type-*A* interface has a Schottky barrier of 0.64 eV, while a type-*B* interface, where the orientation of the silicide is rotated by 180°, has a barrier height of 0.78 eV. Such a single-crystalline and structurally perfect interface² forms an ideal model system for theories of Schottky-barrier formation, allowing for the first time hope for a microscopic understanding based on band-structure calculations.^{3,4} Experimentally, further progress would greatly benefit from the availability of other metal-semiconductor systems having different epitaxial interface structures. Since the discovery of the NiSi₂/Si(111) epitaxy no such system has been reported to date. In this Letter we report on Schottky barriers of the elemental metal lead, grown epitaxially on silicon (111). Two types of contacts, Si(111)(7×7)-Pb and Si(111)(√3×√3)R30°-Pb, can be formed, which differ only in the structure of the first layer of Pb and Si atoms at the interface, while the bulk structures are identical in both cases. The Schottky-barrier heights on *n*-type Si (as determined by capacitance measurements) are 0.70 and 0.93 eV, respectively, differing by as much as 0.23 eV.

The growth of Pb on Si(111) has been studied by several groups.⁵⁻⁹ The system is of particular interest because complications due to chemical reactivity or diffusion are absent. Mutual solid solubility is virtually zero, and there are no stable silicides.¹⁰ The growth follows the Stranski-Krastanov mechanism,⁷ i.e., first one monolayer is completed, and then subsequent growth proceeds in islands. At a coverage of one monolayer two different phases exist at room temperature. Grey *et al.* have determined the atomic structure of both phases using grazing-incidence synchrotron surface x-ray diffraction.⁹ A metastable Si(111)(7×7)-Pb structure is obtained by depositing one monolayer of Pb at room temperature. This structure consists of a two-

dimensional close-packed Pb lattice with 8×8 atoms per Si 7×7 unit cell [Fig. 1(a)]. Heating the sample above 300°C induces an irreversible phase transition to a Si(111)(1×1)-Pb structure. Cooling to room temperature results in a stable Si(111)(√3×√3)R30°-Pb structure. This phase is also close packed, but rotated by 30° with respect to the substrate [Fig. 1(b)], and is incommensurate.⁹ After completion of the first monolayer three-dimensional islands grow in the (111) orientation with Pb[110] parallel to Si[110],⁷ independent of the structure of the adlayer.

The Schottky diodes are fabricated on low-resistivity *n*-type Si(111) wafers with epitaxial layers having a thickness of 6 μm and a resistivity of 2 Ω cm, on which a 400-nm-thick SiO₂ layer is grown. The back of the wafers is implanted with a dose of 1×10¹⁵-cm⁻² 30-keV phosphorus to ensure Ohmic contact. Squares 7×7 mm² are cut from the wafers. On one-half of these squares contact windows of areas ranging from 8.2×10⁻⁵ to 1.6×10⁻³ cm² are defined, while on the other half the oxide is stripped leaving a bare Si surface for monitoring purposes. The samples are cleaned by the Shiraki

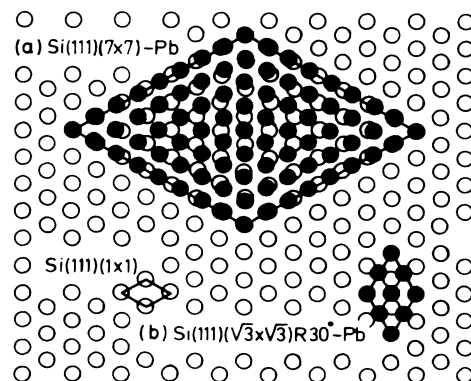


FIG. 1. Atomic arrangement of a Pb monolayer on Si(111): (a) the Si(111)(7×7)-Pb structure; (b) the Si(111)(√3×√3)R30°-Pb structure. A (111) plane of the silicon substrate is shown for reference.

method¹¹ and brought into an ultrahigh-vacuum chamber, which has a base pressure of 10^{-10} mbar. The thin oxide layer in the contact windows is removed by heating the sample from the back with an electron beam for 3 min to about 850°C , as measured with an optical pyrometer. This temperature is low enough to avoid spurious changes in the doping profile.¹²

The surface is studied by Auger electron spectroscopy (AES) and reflection high-energy electron diffraction (RHEED). After the heat treatment no traces of foreign elements can be detected with AES. The bright RHEED patterns show the 7×7 reconstruction of the clean Si(111) surface. The deposition rate is monitored by a quartz-crystal oscillator, which is calibrated with AES, using the joint $\text{Si}(L_{23}MM)\text{-Pb}(N_{67}O_{45}O_{45})$ Auger lines. The deposition rate is 0.12 monolayer/sec.

The first type of Schottky contact [$\text{Si}(111)(7\times 7)\text{-Pb}$] is prepared by evaporating one monolayer of Pb onto the clean $\text{Si}(111)(7\times 7)$ surface, held at room temperature. During deposition the pressure does not exceed 10^{-9} mbar. The Si 7×7 spots in the RHEED patterns gradually become weaker, while the background intensity increases. At the completion of the monolayer only the integer-order and $\frac{6}{7}$ and $\frac{8}{7}$ fractional-order spots remain visible. The increased background indicates imperfections in the ordering at the surface, as can be expected from small relaxations of the structure that are present.⁹ No contamination or compound formation can be detected by RHEED or AES. Further deposition results in the formation of islands with $\text{Pb}[110]$ parallel to $\text{Si}[110]$, which eventually merge into a continuous film. The growth is stopped at a thickness of 500 nm.

The second type of Schottky contact [$\text{Si}(111)(\sqrt{3}\times\sqrt{3})R30^\circ\text{-Pb}$] is prepared by thermal treatment of the sample after the first monolayer has been completed as described above. Heating slowly to 300°C , the fractional-order spots of the metastable adlayer disappear, leaving the 1×1 structure. The sample is held at 300°C for 15 min. Upon cooling a $(\sqrt{3}\times\sqrt{3})R30^\circ$ structure appears below 275°C . Careful analysis of the RHEED data confirms the incommensurability of this phase. The $\text{Pb}(1,0)$ reflection appears at the $(0.65, 0.65)$ position of the $\text{Si}(111)$ reciprocal surface cell. If the hexagonal $\text{Pb}(111)$ were commensurate these spots

TABLE I. Schottky-barrier heights (SBH) of epitaxial Pb/Si(111) contacts. Tabulated values include image-force lowering. For calculating the IV barrier heights an effective Richardson constant of $112 \text{ A/cm}^2\text{K}^2$ was used. Tabulated errors are standard deviations from the mean, obtained from 30 to 40 contacts on several samples.

Interface structure	SBH (eV)	
	IV	CV
$\text{Si}(111)(7\times 7)\text{-Pb}$	0.62 ± 0.02	0.70 ± 0.02
$\text{Si}(111)(\sqrt{3}\times\sqrt{3})R30^\circ\text{-Pb}$	0.90 ± 0.02	0.93 ± 0.01

would appear at the $(\frac{2}{3}, \frac{2}{3})$ position. This result is in excellent agreement with the x-ray analysis by Grey *et al.*⁹ The diffuse background intensity remains strong. Further deposition results in island formation with the same parallel epitaxy as on the 7×7 adlayer. The final film thickness is 500 nm.

Contact pads are defined by etching the Pb in a 2% HF solution, which also serves to remove the native silicon oxide from the back side. Immediately afterwards the back contact is formed by evaporating $0.5\text{-}\mu\text{m}$ aluminum.

Schottky-barrier heights are determined by the capacitance-voltage (CV) and current-voltage (IV) methods at room temperature.¹³ Results are summarized in Table I. Each entry represents 30–40 contacts on different samples. We have reproduced the difference in barrier height in several runs in the course of a year. For the $(\sqrt{3}\times\sqrt{3})R30^\circ$ contacts we sometimes had difficulties fabricating good diodes.

Measured capacitances are frequency independent from 100 kHz to 2 MHz; 400 kHz is taken as the measurement frequency. Typical results for both types of diodes are shown in Fig. 2. The slope of the $1/C^2\text{-}V$ curves corresponds to a doping concentration of $2.7\times 10^{15} \text{ cm}^{-3}$, in agreement with the nominal resistivity. The curves extrapolate to Schottky-barrier heights of $0.70 \pm 0.02 \text{ eV}$ for the $\text{Si}(111)(7\times 7)\text{-Pb}$, and $0.93 \pm 0.01 \text{ eV}$ for the $\text{Si}(111)(\sqrt{3}\times\sqrt{3})R30^\circ\text{-Pb}$ structure. These results are independent of diode size.

The large difference in barrier height is also manifest in the IV measurements (Fig. 3), but some complications arise. The IV curves of the $(\sqrt{3}\times\sqrt{3})R30^\circ$ diodes show

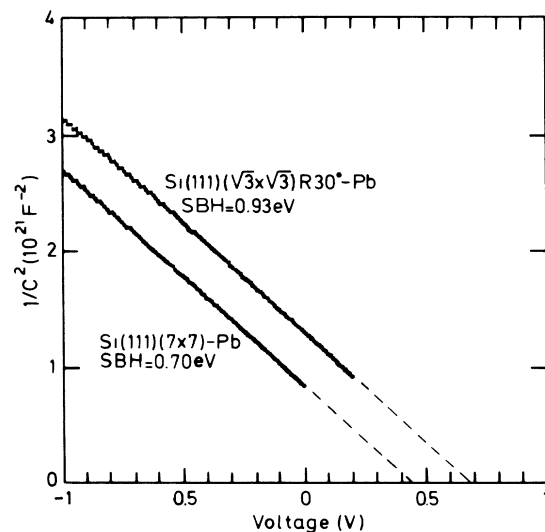


FIG. 2. CV plots of 7×7 and $(\sqrt{3}\times\sqrt{3})R30^\circ$ contacts, measured at 400 kHz. Contact area is $1.6\times 10^{-3} \text{ cm}^2$. The slope of the $1/C^2\text{-}V$ curves corresponds to a doping concentration of $2.7\times 10^{15} \text{ cm}^{-3}$.

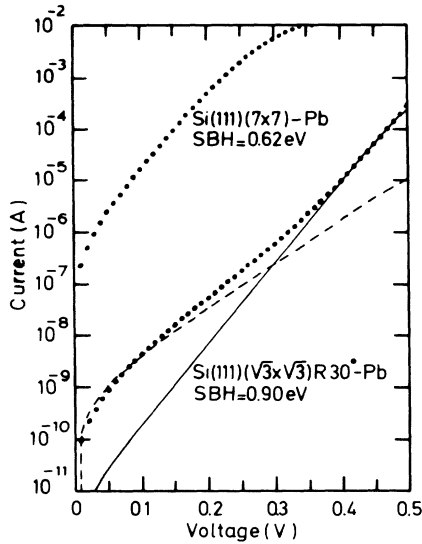


FIG. 3. Forward-current characteristics of 7×7 and $(\sqrt{3}\times\sqrt{3})R30^\circ$ contacts. Contact area is 1.6×10^{-3} cm². For the $(\sqrt{3}\times\sqrt{3})R30^\circ$ curve the fitted thermionic emission current (solid line) and the generation-recombination current (dashed line) are shown.

an excess current of variable magnitude at low forward bias. We attribute this to generation-recombination current originating in the space-charge region, which is a commonly observed phenomenon in high-barrier contacts.^{14,15} One may also consider nonuniformity of the barrier height, e.g., caused by coexistence of the $\text{Si}(111)(\sqrt{3}\times\sqrt{3})R30^\circ\text{-Pb}$ structure with the $\text{Si}(111)(7\times 7)\text{-Pb}$ structure. However, in that case also the barrier height deduced from the CV measurements ought to be lowered. Therefore we have analyzed the forward current with the Schottky-barrier height, the generation-recombination current density, and a series resistance as parameters. Varying the ideality factor between 1.05 and 1.15 does not substantially influence the results. Averaging over all contact sizes we find a Schottky barrier of 0.90 ± 0.02 eV, with generation-recombination current densities ranging from 5×10^{-8} to 5×10^{-7} cm⁻². The barrier height decreases slightly for smaller contact sizes, the difference between the largest and smallest contacts being 0.03 eV. Apparently a small amount of edge current is present, not unexpected considering the very small thermionic emission current in these diodes. The IV curves of the 7×7 diodes show no dependence on contact size, and yield a Schottky barrier of 0.62 ± 0.02 eV, with ideality factors ranging from 1.06 to 1.14.

So both IV and CV methods yield a difference in Schottky-barrier height of at least 0.23 eV between the $\text{Si}(111)(7\times 7)\text{-Pb}$ and the $\text{Si}(111)(\sqrt{3}\times\sqrt{3})R30^\circ\text{-Pb}$ structure. For the $(\sqrt{3}\times\sqrt{3})R30^\circ$ contacts the CV and IV barrier heights agree quite well. For the 7×7 contacts the IV barrier height is significantly lower than the

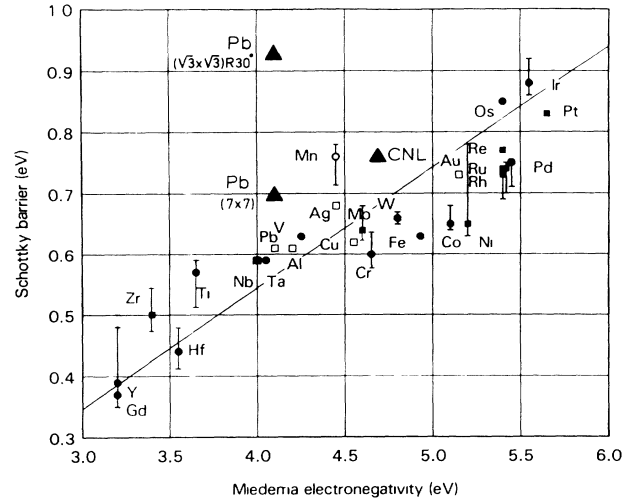


FIG. 4. Schottky-barrier heights of transition-metal silicides and nonreacting metals on n -type silicon [reproduced from Schmid (Ref. 18)]. Solid circles and squares: silicides; open squares: nonreacting metals. The solid line is a linear fit to the data. We have added the present barrier heights for Pb and the charge neutrality level (CNL) from the metal-induced-gap-states theory (Ref. 17), indicated by solid triangles.

CV barrier. This appears to be not unusual for atomically clean contacts on Si, but a conclusive explanation is lacking.¹⁴ The effect has also been observed for Pb on cleaved $\text{Si}(111)$ surfaces by Thanailakis.¹⁶ He has reported barrier heights of 0.72 eV, measured by the CV method, and 0.61 eV by the IV and photoelectric methods. Notably these values almost coincide with our results for the 7×7 contacts.

We will now discuss our results in the light of existing theories of Schottky-barrier formation. First, since the 7×7 and $(\sqrt{3}\times\sqrt{3})R30^\circ$ diodes have identical bulk Si and bulk Pb structures, it is obvious that any theory based solely on bulk properties like work function, electronegativity,¹⁴ or even metal-induced gap states (MIGS)¹⁷ must fail to explain the observed difference in barrier height. Evidently it is caused by a difference in the local electronic structure of the interface. Second, 0.93 eV is an extraordinarily high Schottky barrier, especially for a low-electronegativity metal like Pb ($\chi_{\text{Pb}} = 4.10$ eV on the Miedema scale; $\chi_{\text{Si}} = 4.70$ eV).

These points are brought out more clearly by Fig. 4, which shows Schottky-barrier height versus electronegativity for a collection of elemental metals and silicides on Si. This figure is taken from Schmid,¹⁸ where we have added the present barrier heights for Pb, and the charge neutrality level (CNL) from Tersoff's MIGS theory.¹⁷ According to this theory each semiconductor has its typical, so-called canonical barrier height, which is given by the CNL, the energy where the MIGS cross over from acceptorlike to donorlike character. For n -type Si Tersoff has computed a canonical barrier height of 0.76 eV. Deviations from this value must follow linearly the elec-

tronegativity difference. This behavior is roughly borne out by the data shown in Fig. 4. The 0.70- (0.62-) eV barrier height of our 7×7 contacts conforms reasonably to the general trend, but it is clear that the 0.93-eV barrier height of the $(\sqrt{3}\times\sqrt{3})R30^\circ$ contacts cannot be explained within this model.

Apparently interface states of a different origin are involved. Calculations of Zur, McGill, and Smith indicate that it takes on the order of 10^{14} interface states per cm^2 to pin the Fermi level for thick, metallic coverages.¹⁹ Therefore the barrier height of the $\text{Si}(111)(\sqrt{3}\times\sqrt{3})R30^\circ$ -Pb structure requires a high density of states in the lower part of the band gap, at or below 0.93 eV below the conduction-band edge. The origin of these states must reside in the bonding details of the Pb and Si atoms that constitute the interface. Since there is an ordered atomic arrangement at the interface it is perfectly conceivable that an intrinsic electronic state of the required areal density exists at a discrete energy level. However, since there is a detectable level of disorder in the interface structure, the possibility that such a state is related to a particular kind of structural defect cannot be ruled out.

A comparison with the $\text{Si}(111)(7\times 7)$ -Pb interface is complicated by the fact that here the silicon lattice may still be terminated by the 7×7 reconstruction, instead of an unreconstructed (111) plane. The $\text{Si}(111)(7\times 7)$ -Pb interface is also ordered, and a discrete intrinsic interface state could exist as well. Electrical transport measurements are unable to resolve this matter.

The authors have enjoyed stimulating discussions with F. Grey and J. Vrijmoeth, and thank J. W. Wensink for assistance with the experiments. This work is part of the research program of the Stichting voor Fundamenteel Onderzoek der Materie (FOM) and the Stichting voor Scheikundig Onderzoek Nederland (SON), which are financially supported by the Nederlandse Organisatie

voor Wetenschappelijk Onderzoek (NWO).

^(a)Present address: Physics Laboratory, University of Groningen, Westersingel 34, 9718 CM Groningen, The Netherlands.

¹R. T. Tung, Phys. Rev. Lett. **52**, 461 (1984).

²R. T. Tung, J. M. Gibson, and J. M. Poate, Phys. Rev. Lett. **50**, 429 (1983).

³X. Yongnianan, Z. Kaining, and X. Xide, Phys. Rev. B **33**, 8602 (1986).

⁴G. P. Das, P. Blöchl, O. K. Andersen, N. E. Christensen, and O. Gunnarsson, Phys. Rev. Lett. **63**, 1168 (1989).

⁵P. J. Estrup and J. Morrison, Surf. Sci. **2**, 465 (1964).

⁶M. Saitoh, K. Oura, K. Asano, F. Shoji, and T. Hanawa, Surf. Sci. **154**, 394 (1985).

⁷G. LeLay, J. Peretti, and M. Hanbücken, Surf. Sci. **204**, 57 (1988).

⁸H. Yaguchi, S. Baba, and A. Kinbara, Appl. Surf. Sci. **33/34**, 75 (1988).

⁹F. Grey, R. Feidenhans'l, M. Nielsen, and R. L. Johnson, J. Phys. (Paris) **50**, 7181 (1989).

¹⁰R. W. Olesinski and G. J. Abbaschian, Bull. Alloy Phase Diagrams **5**, 271 (1984).

¹¹A. Ishizaki and Y. Shiraki, J. Electrochem. Soc. **133**, 666 (1986).

¹²R. T. Tung, K. K. Ng, J. M. Gibson, and A. F. J. Levi, Phys. Rev. B **33**, 7077 (1986).

¹³S. M. Sze, *Physics of Semiconductor Devices* (Wiley, New York 1981), 2nd ed.

¹⁴E. H. Rhoderick and R. H. Williams, *Metal-Semiconductor Contacts* (Clarendon, Oxford, 1988), 2nd ed.

¹⁵I. Ohdomari, K. N. Tu, F. M. d'Heurle, T. S. Kuan, and S. Petersson, Appl. Phys. Lett. **33**, 1028 (1978).

¹⁶A. Thanailakis, J. Phys. C **8**, 655 (1975).

¹⁷J. Tersoff, Phys. Rev. Lett. **52**, 465 (1984).

¹⁸P. Schmid, Helv. Phys. Acta **58**, 371 (1985).

¹⁹A. Zur, T. C. McGill, and D. L. Smith, Phys. Rev. B **28**, 2060 (1983).